International Journal of Heat and Technology
Vol. 39, No. 6, December, 2021, pp. 1791-1798
Journal homepage: http://iieta.org/journals/ijht

Effect of Silica Oxide SiO_2/Water Nanofluids Volume Concentration Ratio on Photovoltaic Thermal (PVT) Collector Efficiency

Wan Mustafa[1,2*], Ahmad Fudholi[2,3], Kamaruzzaman Sopian[2], Jasrina Jaafar[1], Muslizainun Mustapha[2]

[1] Water and Energy Department, Universiti Kuala Lumpur Malaysia France Institute, Selangor 43650, Malaysia
[2] Solar Energy Research Institute (SERI), Universiti Kebangsaan Malaysia, Selangor 43650, Malaysia
[3] Research Centre for Electrical Power and Mechatronics, Indonesian Institute of Sciences (LIPI), Bandung 12710, Indonesia

Corresponding Author Email: wanmustafa@unikl.edu.my

https://doi.org/10.18280/ijht.390612

Received: 19 August 2021
Accepted: 2 December 2021

Keywords:
photovoltaic thermal, spiral heat collector, nanofluids, thermal efficiency, electrical efficiency

ABSTRACT

The main challenge for photovoltaic systems is to withstand the high surface and ambient temperatures caused by direct solar radiation, which decreases system efficiency. This research aims to develop a photovoltaic thermal system cooling method using nanofluid SiO_2/water with a volume concentration of 0.5-1.5 vol.% and a radiation rate of 450-850W/m^2. The working fluid flow rate is between 1.8 and 6 L/min at each radiation rate. SiO_2/water 1.5 vol.% under 850W/m^2 radiation with a flow rate of 6 L/min produced the best results, with an average overall efficiency of 71.99%, the thermal efficiency of 63.43%, and electrical efficiency of 8.56%. However, the highest electrical energy efficiency was achieved at 650W/m^2 with a 9.27% efficiency.

1. INTRODUCTION

The degradation of silicon-based PV performance due to dust deposition on the surface, shading, and temperature rise reduces the total efficiency of the PV system, has a significant impact on the economic aspect, and is an essential element of widely used silicon-based photovoltaic [1]. The simple ageing of PV panels can cause performance deterioration, typically ranging from 0.5% to 1.0% each year and is heavily dependent on individual climatic conditions [2]. Different cooling techniques, which can be passive or active, have been investigated in recent years to decrease the unfavourable effects of higher operating temperatures on the overall performance of PV systems.

A photovoltaic thermal system (PVT) is primarily a typical photovoltaic panel that converts solar energy into electrical energy. A thermal collector absorbs surplus photon energy and heat produced by photovoltaic cells [3]. The hybrid PVT collector concept was created to improve PV panel performance by using the cooling effects of thermal collectors [4]. PVT collectors are highly helpful because they can convert more solar energy than flat plate solar collectors with the same opening region. The performance of the PV panel reduces as the surface temperature rises. At the same time, the thermal collector portion acts as a heat absorber from the solar energy radiation that strikes the PV panel's surface.

These sorts of solar systems are more efficient than traditional PV modules since they generate both electricity and valuable heat energy at the same time. Increasing the surface temperature of the PV unit reduces its electrical efficiency by almost 0.45% for each degree of temperature rise [5]. Various PVT manufacturing processes have been explored and implemented worldwide in the past. However, few studies tried to glue PV cells into thermal absorbers directly, and even fewer tried to incorporate commonly available PV modules into thermal absorber or heat extraction systems. The most common and primary approach in manufacturing PVT collectors is to apply thermal paste on heat collector absorbers [6]. This thermal paste acts as a filler for the air gap trapped between the PV panel and the absorber while increasing the heat transfer rate between these two surfaces. Water-based heat transfer fluid systems are the most preferred PVT systems because they offer better overall efficiencies than air-based systems and allow more constant cooling of PV cells [7]. The coolant channel flow distribution determines the effectiveness of PVT collectors [8].

The channel design should enhance heat transfer and retain heat more efficiently from the collector to the heat transporting fluid. Many investigators have used novel cooling techniques to improve the performance of PVT liquid collectors, a few of which are highlighted below. For example, Ji et al, created a photovoltaic aluminium alloy flat box for a natural circulation water heating system. For 0.63 PV cell covers and 0.83 front glazing transmissivity, total daily energy, thermal efficiency, and electrical efficiency were 52%, 45% and 10.15%, respectively [9]. At Hong Kong City University, He et al. measured a daily PVT thermal efficiency of 40% in an aluminum alloy channel utilizing water as the heat transfer fluid [10].

Fraisse et al. [11] investigated four distinct PVT device designs for construction applications. The four designs separated PV and thermal systems, covered hybrid PVT systems, uncovered hybrid PVT systems, and covered PVT systems with low glass emissivity. The annual cell efficiency of the covered PVT system was recorded to be 6.8% lower than the typical non-integrated PV cell efficiency of 9.4% [11]. Yazdanifard et al. [12] developed a water-based flat plate PVT system simulation. The researchers focused on how solar radiation, packing factor, Reynolds number, collector length, pipe diameter and pipe number influenced the system's

performance. The average electrical efficiency was 11.5%, while the highest thermal efficiency achieved was 70%. Several studies focused on a nanofluid consisting of the foundation fluid of water/water/ethylene glycol nanomaterial. Using nanoscale materials and suitable mixing with the base fluids resulted in a remarkable increase in the thermal properties and performance combination.

This improvement is directly related to nanoparticles' composition, size, and concentration [13]. Therefore, this study conceived and developed a stainless steel spiral absorber in water and a nanofluid-based PVT system. This experiment was conducted in a solar simulator with three different radiation levels: 850W/m^2, 650W/m^2 and 450W/m^2. The working fluid comprises water and SiO_2/water nanofluid in 0.5 vol.%, 1.0 vol.% and 1.5 vol.%, respectively.

2. EXPERIMENT SETUP

2.1 Spiral collector and indoor simulator setup

The PVT water collector was tested in the Sustainable Energy Analysis Laboratory, Universiti Kuala Lumpur Malaysia France Institute. At this facility, the solar simulator is made up of 28 halogen tungsten lamps, each with an output power of 500 W. The lamps are set for each column in seven columns of 4 lamps, as shown in Figure 1. The irradiance can be adjusted using a sliding manual voltage regulator to adjust the voltage input to the halogen simulator (Carrol & Meynell Ltd). This experiment used three different radiations (850 W/m^2, 650W/m^2, 450 W/m^2) to determine PVT performances under different climates. Control parameters for indoor testing include temperatures of inlet and outlet collector, ambient temperature, wind velocity, output current, voltage and liquid flow rate inside the tube.

Table 1. Design parameters of a PVT system

Photovoltaic panel (STC)	
Type	Monocrystalline silicon
Rated power (W)	100 Wp
Panel dimension (cm)	820 x 808
Number of cells	36
Open circuit voltage, V_{oc} (V)	22.53V
Maximum voltage, V_{mp} (V)	18.75 V
Maximum current, I_{mp} (A)	5.35 A
Short circuit current (A)	5.70 A
Panel efficiency	15.1%
PVT collector	
Type	Spiral square tube
Material	Stainless steel
Tube thickness	1 mm
Inner tube diameter	10 mm
Outer tube diameter	12 mm
Insulation thickness	10 mm

The photovoltaic panel used in this study is composed of monocrystalline silicon with a rated power of 100W. Figure 2 shows a spiral tube collector used as a heat collector, and the specifications of this collector can be referred to in Table 1.

The heat collector consisted of stainless steel square tubes arranged in spiral flow and welded using an inert tungsten gas (TIG) welding. The spiral flow heat collector without an absorber plate was inserted to the bottom side of the PV module using a high-temperature silicone adhesive and sealant. Beneath the heat collector, the thermal insulator was affixed to prevent more heat from escaping and provide more consistent temperatures. The heat collector was designed as a continuous coil or shaped tube composed of at least one inlet and outlet to allow the working fluid to enter and exit a heat collector [14]. The inlet and outlet fittings were positioned to allow working fluid to flow into and out of the heat collector and exits as hot water.

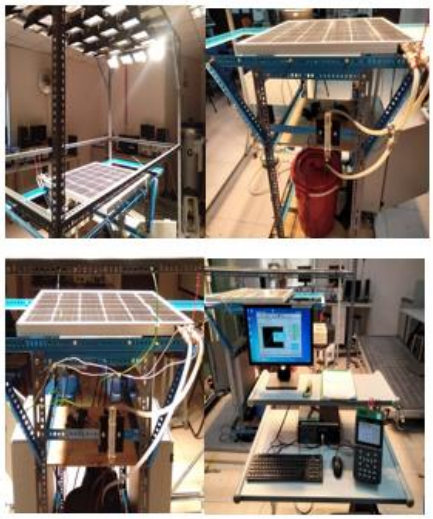

Figure 1. PVT experimental indoor setup

Figure 2. Spiral heat collector

Using three different concentrations of SiO_2/water (0.5 vol.%, 1.0 vol.%, and 1.5 vol.%), each of which is stored in a tank (20 litre capacity). Two surface pumps (DC 12V 70W) were installed in a parallel configuration to distribute the fluid around the panel at flow rates of 6L/min, 4.6L/min, 3.2L/min, and 1.8L/min, respectively.

A variable flow meter (0.0-10.0L/min) is used to measure flow rates at the inlet and outlet of the collector. The flow temperatures at the collector inlet and outlet and the PV surface temperature are measured and saved with a data logger (Omron ZR-RX45) by K-type thermocouples. A solar module analyzer (Prova 200A) measures PVT module characteristics such as voltage, current and power. The experiment was tested for 60 minutes, and the data was recorded for every 1-minute interval for all water and SiO_2/water.

PVT system evaluated at temperatures and solar radiation levels equivalent to those used during PV module tests in a laboratory. This indoor experiment is based on several assumptions.

1. Irradiance and wind speed following the original conditions during the experiment are considered stable.
2. Water constantly flows towards water flow at consistent input water temperatures.

3. NANOFLUIDS PROPERTIES

3.1 Thermal conductivity and viscosity

Sharma et al. [15] used experimental data from several investigators to create equations for estimating viscosity and thermal conductivity for water-based nanofluids, given by Eqns. (1) and (2), respectively. The equations are valid for concentrations of less than 4%, liquid temperatures of 70°C, and diameters of 170 nm. The equations can estimate the characteristics of metal and metal oxide nanofluids distributed in the water. The measured viscosity and thermal conductivity values correspond well with the values calculated using Eqns. (1) and (2) and utilized in the analysis. For thermal conductivity and viscosity, the difference between experimental data and the values predicted by Eqns. (1) and (2) is less than 1% and 5%, respectively.

$$\frac{\mu_{nf}}{\mu_w}=\left(1+\frac{\phi}{100}\right)^{11.3}\left(1+\frac{T_{nf}}{70}\right)^{-0.038}\left(1+\frac{d_p}{170}\right)^{-0.061} \tag{1}$$

$$\frac{k_{nf}}{k_w}=0.8938\left(1+\frac{\phi}{100}\right)^{1.37}\left(1+\frac{T_{nf}}{70}\right)^{0.2777} x\left(1+\frac{d_p}{150}\right)^{-0.0336}\left(\frac{\alpha_p}{\alpha_w}\right)^{0.01737} \tag{2}$$

Table 2 shows the thermal diffusivity of Al_2O_3, TiO_2 and SiO_2 nanoparticles and their ratio to water at 30°C.

Table 2. Thermal diffusivity ratio

Nanofluid	Particle thermal diffusivity, α_p x 10^7	Thermal diffusivity ratio, α_p/α_w
Al_2O_3	120.03	81.19
TiO_2	28.69	19.41
SiO_2	8.46	5.73

3.2 Density and specific heat

A small percentage of solid nanoparticles added to a base liquid would gradually increase the density of the mixture [16]. This is because solids have a higher density than liquids. Therefore, density modelling in nanofluids needs an assessment of the constituents' material densities and volume concentrations. The density of nanofluids has been studied for various particle sizes (1–100 nm), temperatures (5–60°C), and volume concentrations (0–5.0 vol.%). For example, Ho et al. [17] reported a 10% rise in Al_2O_3/water nanofluid density at 4% vol. However, when the density of the nanofluid dropped by 5% and the temperature rose from 25 to 40°C. The following is a description of the effective density of nanofluid ρ_{nf} based on standard mixing theory:

$$\rho_{nf}=\phi_p\rho_p+\left(1-\phi_p\right)\rho_w \tag{3}$$

where, ρ_{nf} is the effective density of the nanofluid and the ϕ_p volume fraction percentage of nanoparticles. When the materials are in thermal equilibrium, nanofluid specific heat may be represented as a combination of the heat capacities of solid and liquid phases. Xuan and Roetzel [18] proposed an equation for estimating the specific heat of a nanofluid, which is given by:

$$C_{nf}=\frac{\left(1-\phi_p\right)\left(\rho_w C_w\right)+\rho_p C_p\phi_p}{\rho_{nf}} \tag{4}$$

where, C_p is the specific heat, ρ_p is the density, ϕ_p is the volume fraction of the nanoparticle, and ρ_{nf} is the predicted nanofluid density using Eq. (3) and the nanoparticle properties given in Table 3.

Table 3. Nanoparticle and base fluid properties

	k (W/m K)	ρ (kg/m^3)	C (J /kg K)	μ (P.as)
Water	0.609	997	4180	0.00089
SiO_2	1.4	2220	745	-

4. ANALYSIS OF PVT COLLECTOR

4.1 Thermal efficiency

PVT thermal efficiency, η_{th} is defined as:

$$\eta_{th}=\frac{Q_u}{Q_s} \tag{5}$$

where, Q_u is useful to heat absorbed by the PVT collector and can be expressed as a function of mass flow rate (m), working fluid heat capacity (C_p), and temperature difference between the PVT collector's inlet and outlet, it is written as:

$$Q_u=\dot{m}C_p\left(T_o-T_i\right) \tag{6}$$

From Eq. (5), the thermal efficiency can be expanded as [19]:

$$\eta_{th}=F_R\left[(\tau\alpha)_{pv}-U_L\left(\frac{T_i-T_a}{G_t}\right)\right] \tag{7}$$

where $(\tau\alpha)_{pv}$ is PV thermal efficiency, U_L is the overall loss for the PVT collector, the sum of edge, U_e back loss, U_b and top loss, U_t [20], and F_R is the heat removal factor.

$$U_L=U_e+U_b+U_t \tag{8}$$

$$U_t=\left[\frac{N_g}{\left(\frac{C}{T_{pm}}\right)\left(\frac{T_{pm}-T_a}{N_g+f}\right)^{0.33}+\frac{1}{h_w}}\right]^{-1} +\frac{\sigma\left(T_a+T_{pm}\right)\left(T_a^{\,2}+T_{pm}^{\,2}\right)}{N_g+\frac{1}{\varepsilon_p+0.05N_g\left(1-\varepsilon_p\right)}+\frac{2N_g+f-1}{\varepsilon_g}} \tag{9}$$

$$f = \left(0.0005h_w{}^2 - 0.04h_w + 1\right)\left(0.091N_g + 1\right) \quad (10)$$

$$C = \left(0.0001298\beta^2 - 0.00883\beta + 1\right)365.9 \quad (11)$$

The energy lost from the collector's bottom is initially carried through the insulation before being transferred to the surrounding through a combination of convection and infrared radiation. The heat loss from the collector via the rear of the collector is governed by the conduction resistance of the collector rubber insulation mat.

$$U_b = \left(\frac{t_b}{k_b} + \frac{1}{h_{c,b-a}}\right)^{-1} \quad (12)$$

$$U_e = \left(\frac{t_a}{k_a} + \frac{1}{h_{c,e-a}}\right)^{-1} \quad (13)$$

In this study, back and edge materials are composed of the same material and dimension then ($t_e = t_b$) insulation thickness and ($k_e = k_b$) insulation thermal conductivity. The back surface ($h_{c,b-a}$) and edge loss coefficients ($h_{c,e-a}$) can be taken as (0.3-0.6 W/m^{2}K) and (1.5–2 W/m^{2}K) [19].

Heat removal factor, F_R introduced by Duffie et al. [20] is expressed as follows:

$$F_R = \frac{\dot{m}C_p}{A_c U_L}\left[1 - \exp\left(\frac{-A_c U_L F'}{\dot{m}C_p}\right)\right] \quad (14)$$

where, F' is the collector efficiency factor, which is determined by using:

$$F' = \frac{\left(\frac{1}{U_L}\right)}{W\left\{\frac{1}{[F(W-D)+D]U_L} + \frac{1}{C_b} + \frac{1}{\pi h_{fi} D_h}\right\}} \quad (15)$$

D_h is the hydraulic diameter of the collector tube, C_b is the thermal grease conductance, h_{fi} is the working fluid heat transfer coefficient, D is the diameter of the collector tube, W is the spacing between the collector tubes, and F is the fin efficiency factor, which is given as:

$$F = \frac{\tanh\left[(W-D)(0.5M)\right]}{\left[(W-D)(0.5M)\right]} \quad (16)$$

Coefficient M is calculated using:

$$M = \sqrt{\frac{U_L}{k_{pv}\delta_{pv} + k_c\delta_c}} \quad (17)$$

where, k_{pv} and k_c are the thermal conductivities of the PV panel and collector, and δ_{pv} *and* δ_c are the thicknesses of the PV panel and collector.

4.2 Electrical efficiency

PVT electrical efficiency is defined as:

$$\eta_e = \frac{P_{mp}}{A_{pv}G_t} = \frac{V_{mp}\,\mathrm{I}_{mp}}{A_{pv}G_t} \quad (18)$$

I_{mp} is the maximum current, P_{mp} is the maximum electrical power, V_{mp} is the maximum voltage. These values were measured using a solar module analyzer at intervals of every 1 minute.

5. RESULTS AND OBSERVATIONS

5.1 PVT/water thermal efficiency analysis

Figure 2 depicts increasing thermal efficiency as flow rate increases from 1.8L/min to 6L/min under solar radiation ranging from 450W/m^2 to 850W/m^2. It was discovered that when flow rates increased, the thermal efficiency rose from 41.53% to 43.09%, with an average value of 42.37% as the solar radiation adjusted to 450W/m^2. This rising trend demonstrates a 3.62% increase. The water flow rate factor aids this increase in thermal efficiency. By adjusting the water flow rate from 1.8L/min to 6L/min, the surface temperature of the PV panel will decrease due to the heat transfer carried by the water, and subsequently, the output temperature will increase. At 850W/m^2 radiation, the experimental results show the highest thermal efficiency. The thermal efficiency measured ranges from 47.94% to 50.46%, with an average efficiency of 49.36% and a percentage increase of 4.99%. At 650W/m^2, the resulting thermal efficiency ranges from 47.40% to 50.51%, with an average efficiency of 48.98%. All experiments showed the highest thermal efficiency at a flow rate of 6 L/min.

In summary, Figure 3 illustrates the relationship between water flow rate and thermal efficiency as a function of solar radiation intensity. When radiation levels increase, the amount of energy and temperature absorbed by the photovoltaic module will also increase. As the temperature rises, the heat transfer from the PV to the working fluid increases, thus increasing the working fluid's output temperature.

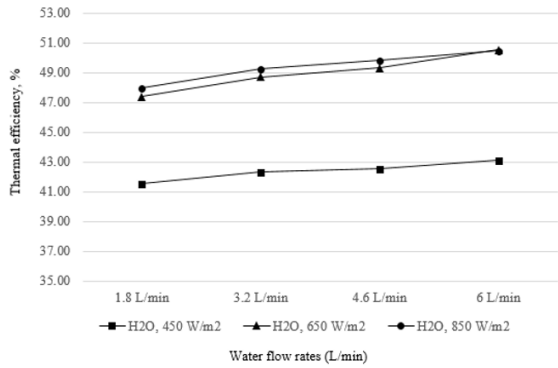

Figure 3. PVT/water thermal efficiency with different flow rates and solar irradiances

5.2 PVT/water electrical efficiency analysis

Figure 4 depicts the average electrical efficiency versus flow rates ranging from 1.8 to 6L/min and solar radiation ranging from 450 to 850W/m^2. At a flow rate of 6L/min, the average electrical efficiency was the highest. Solar radiation and working fluid flow rate will impact the electrical performance of the PVT. The studies also demonstrate that the electrical efficiency increased when the cell temperature

decreased. This is because the heat generated on the PV panel and the heat collector will be removed by the water flowing through the tube, lowering the temperature of the PVT/water cell. As a result, the temperature will drop, and the electrical efficiency will increase. Figure 4 shows that at 850W/m^2, the electrical efficiency attained is the lowest, with a maximum efficiency of 8.2% observed. The average electrical efficiency was 8.1%, with a 2.16% enhancement.

The rising trend is more or less the same at 650W/m^2 and 450W/m^2, where the highest efficiency was recorded at 8.98% and 8.8%, respectively, while the average efficiency is the same at 8.73%. In comparison, the efficiency achieved is almost equal due to several factors:

(a) The level of solar radiation

The adjusted solar radiation level could not be adjusted to the exact value in the experiments.

(b) Temperature

The surface temperature is slightly higher because this temperature is generated by the solar simulator, which is more focused on the photovoltaic panel surface.

The electrical efficiency performance at 650W/m^2 radiation, on the other hand, is regarded the greatest since it achieved the most significant percentage enhancement of 5.39% compared to 3.02%.

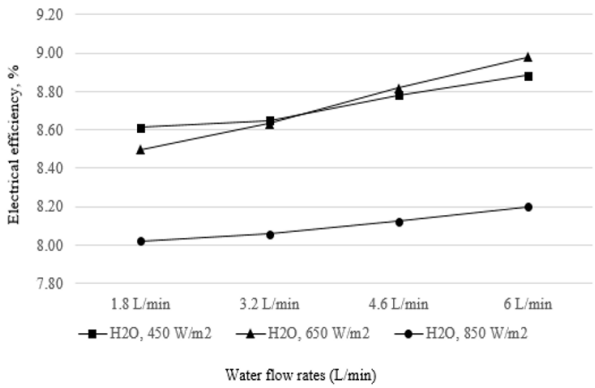

Figure 4. PVT/water electrical efficiency with different flow rates and solar irradiances

5.3 Thermal efficiency analysis of PVT SiO_2/water nanofluids

Figure 5 shows the thermal efficiency performance of a PVT collector by using SiO_2/water nanofluids as the working fluid. The comparative study was conducted on differences in volume concentration of 0.5 vol.%, 1.0 vol.%, and 1.5 vol.%. The volume concentration of 1.5 vol.% recorded the most outstanding results at 850W/m^2 of radiation, with the maximum thermal efficiency of 64.16% and average efficiency of 63.43%. The same increasing thermal efficiency trend occurs at 1.0 vol.% and 0.5 vol.%. Thermal efficiency ranged from 59.2% to 62.2% at 1.0 vol.% volume concentration, with an average efficiency of 60.71% achieved. While at 0.5 vol.%, it was found that the thermal efficiency decreased slightly with a range of 49.42% to 52.18%. The average thermal efficiency was 50.79% when the flow rate changed from 1.8L/min to 6L/min.

The experiment was conducted with the radiation level reduced to 650W/m^2. Under these conditions, the volume concentration of 1.5 vol.% still achieved the maximum thermal efficiency. The thermal efficiency increased from 58.98% to 61.69% due to the adjustment in flow rate. The thermal efficiency attained at a volume concentration of 1.0 vol.% varied from 51.38% to 53.31%, with an average efficiency of 52.37%. While at 0.5 vol.%, the thermal efficiency dropped from 48.2% to 51.5%, with an average efficiency of 49.9%. Compared to water performance, the maximum efficiency enhancement percentage is 11.43% at a volume of 1.5 vol.%.

The average thermal efficiencies obtained at 1.5 vol.%, 1.0 vol.%, and 0.5 vol.% at 450W/m^2 radiation were 56.8%, 51.42% and 46.98%, respectively. It is possible to make an overall comparison that 1.5 vol.% volume concentration with a flow rate of 6L/min and solar radiation of 850W/m^2 were significant factors for optimal thermal efficiency performance. This parameter is a good fit for spiral heat collectors. Apart from the intensity of solar radiation and the flow rate of the working fluid, this phenomenon can be attributed to the high thermal properties of SiO_2/water compared to the lower thermal properties of water. The volume concentration ratio of SiO_2/water at 1.5 vol.%, exhibits high thermal conductivity properties compared to 0.5 vol.%, 1.0 vol.% SiO_2/water and pure water, which will increase the high heat transfer rate and increase the thermal efficiency.

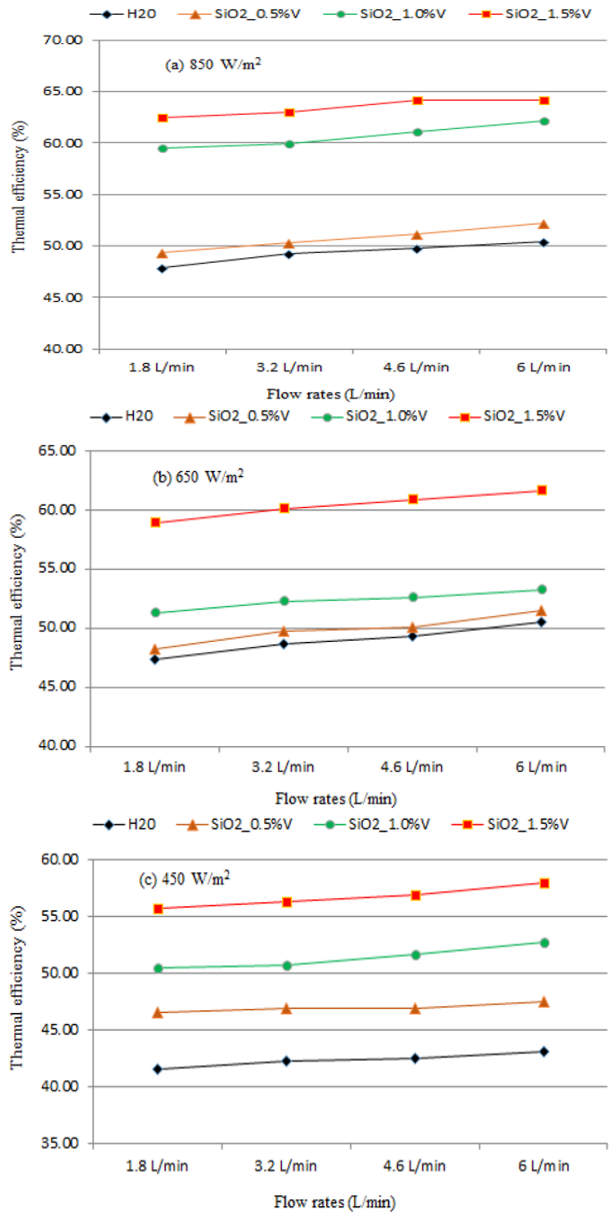

Figure 5. PVT SiO_2/water thermal efficiency with different flow rates, volume concentrations and solar irradiances

5.4 Electrical efficiency analysis of PVT SiO_2/water nanofluids

The surface temperature of the PVT panel and the solar radiation rate will impact the electrical efficiency. The cooling technique can lower the surface temperature of the PVT panel while also increasing its electrical efficiency.

Figure 6 depicts the performance of the electrical efficiency with SiO_2/water as the working fluid. The highest average electrical efficiency was observed at 9.27% for a volume concentration of 1.5 vol.%, which is at a radiation level of 650W/m^2, followed by 8.92% and 8.56% for radiation levels of 450W/m^2 and 850W/m^2, respectively. At the same time, the maximum efficiency is reached for all radiation levels at a flow rate of 6L/min.

At a volume concentration of 1.0 vol.%, the electrical efficiency decreased slightly. At this stage, the highest average efficiency is 9.09% with 650W/m^2 radiation, followed by 8.86% at 450W/m^2. Finally, the average efficiency at 850W/m^2 radiation is 8.47%, the lowest at a volume concentration of 1.0 vol.%.

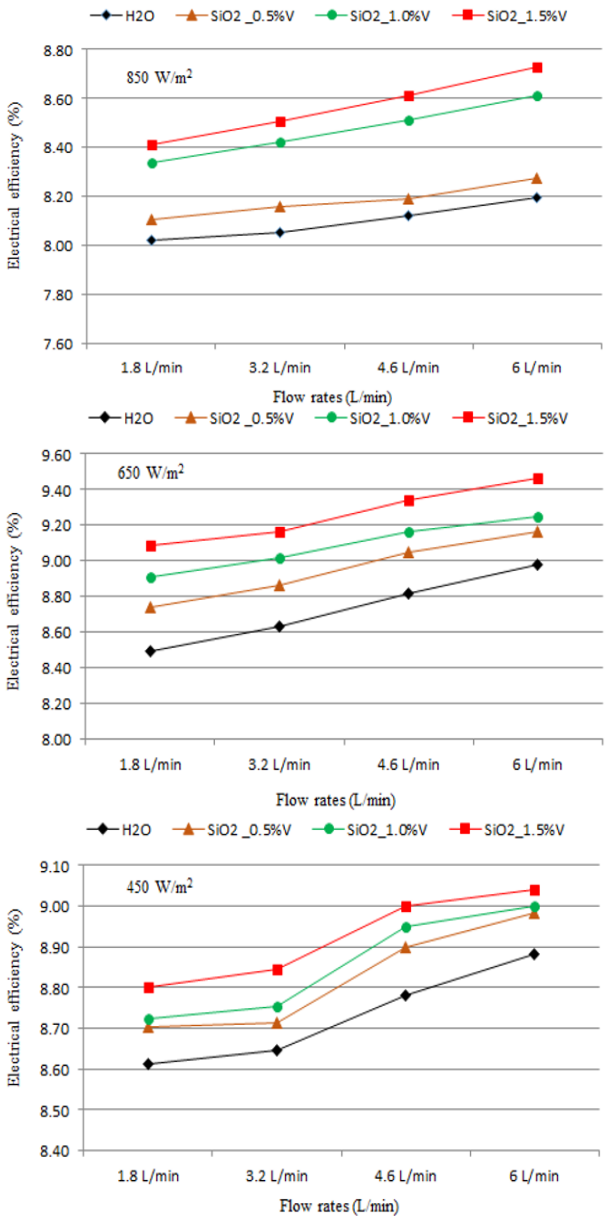

Figure 6. PVT SiO_2/water electrical efficiency with different flow rates, volume concentrations and solar radiations

The lowest average electrical efficiencies were 8.18% at 850W/m^2 and 8.95%, 8.82%, and 8.82%, respectively, at 650W/m^2 and 450W/m^2. All of this occurred at a volume concentration of 0.5 vol.%. According to the electrical efficiency performance, high volume concentration increased the electrical efficiency. This performance-enhanced 5.37%, 5.82%, and 2.13% compared to water. At radiation rates of 850W/m^2, 650W/m^2 and 450W/m^2, the highest electrical efficiency enhancement were 6.07%, 5.17% and 1.77% respectively. Figure 6 shows that the cooling effect of the collector is related to changes in electrical efficiency. As a result of this research, it has been demonstrated that nanofluids with improved thermal conductivity can absorb more heat from solar panels than water, resulting in increased output power and efficiency.

Table 4 shows the total efficiency of PVT SiO_2/water nanofluids. With increasing radiation intensities from 450W/m^2 to 850W/m^2, SiO_2/water 1.5 vol.% demonstrated the highest total efficiency range from 65.72% to 71.99%.

Table 4. The total average efficiency of PVT SiO_2/water nanofluids

	850 W/m^2	650 W/m^2	450 W/m^2
	η_t	η_t	η_t
SiO_2/water 1.5 vol.%	71.99%	69.68%	65.72%
SiO_2/water 1.0 vol.%	69.18%	61.46%	60.28%
SiO_2/water 0.5 vol.%	58.97%	58.85%	55.80%
water	57.46%	57.71%	51.10%

6. CONCLUSIONS

PVT collector system was investigated experimentally using water and SiO_2/water with volume concentrations of 0.5 vol.%, 1.0 vol.% and 1.5 vol.% as working fluids. All of the study's findings were compared to the performance of water as a working fluid. Compared to the water-based system, the PVT system employing nanofluids demonstrated a significant increase in electrical and thermal efficiency. Furthermore, the findings show that a high volume concentration of nanofluid enhances heat transfer rate and nanofluid attributes are better than water.

The electrical and thermal efficiency of PVT collectors is influenced by the thermophysical characteristics of SiO_2/water nanofluids. Because of the thermal conductivity properties of nanoparticles, the heat transfer coefficient can be increased.

Thermal and electrical efficiency performance with different working fluids, volume concentrations, radiation rates, and flow rates were determined. According to the study's findings, a radiation level of 850W/m^2 and a flow rate of 6 L/min with SiO_2/water 1.5 vol.% could contribute to an average overall efficiency of 71.99%, a thermal efficiency 63.43%, and electrical efficiency of 8.56%. However, at a radiation level of 650W/m^2, the maximum electrical efficiency of 9.27% was recorded. It was verified in this investigation that adding nanoparticles to the base fluid enhanced the heat transfer characteristics. Therefore, it has also been proposed that nanofluids improve the efficiency of PVT systems by increasing heat transfer.

ACKNOWLEDGMENT

The author would like to thank the Sustainable Energy

Analysis Laboratory (SEAL), Universiti Kuala Lumpur Malaysia France Institute, for providing the laboratory facilities and technical support.

REFERENCES

[1] Marinić-Kragić, I., Nižetić, S., Grubišić-Čabo, F., Čoko, D. (2020). Analysis and optimization of passive cooling approach for free-standing photovoltaic panel: Introduction of slits. Energy Conversion and Management, 204: 112277. https://doi.org/10.1016/j.enconman.2019.112277

[2] Jordan, D.C., Kurtz, S.R., VanSant, K., Newmiller, J. (2016). Compendium of photovoltaic degradation rates. Progress in Photovoltaics: Research and Applications, 24(7): 978-989. https://doi.org/10.1002/pip.2744

[3] Sardarabadi, M., Hosseinzadeh, M., Kazemian, A., Passandideh-Fard, M. (2017). Experimental investigation of the effects of using metal-oxides/water nanofluids on a photovoltaic thermal system (PVT) from energy and exergy viewpoints. Energy, 138: 682-695. http://dx.doi.org/10.1016/j.energy.2017.07.046

[4] Yandri, E. (2019). Development and experiment on the performance of polymeric hybrid Photovoltaic Thermal (PVT) collector with halogen solar simulator. Solar Energy Materials and Solar Cells, 201: 110066. http://dx.doi.org/10.1016/j.solmat.2019.110066

[5] Bai, A., Popp, J., Balogh, P., Gabnai, Z., Pályi, B., Farkas, I. (2016). Technical and economic effects of cooling of monocrystalline photovoltaic modules under Hungarian conditions. Renewable and Sustainable Energy Reviews, 60: 1086-1099. https://doi.org/10.1016/j.rser.2016.02.003

[6] Sandnes, B., Rekstad, J. (2002). A photovoltaic/thermal (PV/T) collector with a polymer absorber plate. Experimental study and analytical model. Solar Energy, 72(1): 63-73. http://dx.doi.org/10.1016/S0038-092X(01)00091-3

[7] Herrando, M., Markides, C.N., Hellgardt, K. (2014). A UK-based assessment of hybrid PV and solar-thermal systems for domestic heating and power: System performance. Applied Energy, 122: 288-309. https://doi.org/10.1016/j.apenergy.2014.01.061

[8] Weitbrecht, V., Lehmann, D., Richter, A. (2002). Flow distribution in solar collectors with laminar flow conditions. Solar Energy, 73(6): 433-441. https://doi.org/10.1016/S0038-092X(03)00006-9

[9] Ji, J., Lu, J.P., Chow, T.T., He, W., Pei, G. (2007). A sensitivity study of a hybrid photovoltaic/thermal water-heating system with natural circulation. Applied Energy, 84(2): 222-237. https://doi.org/10.1016/j.apenergy.2006.04.009

[10] He, W., Chow, T.T., Ji, J., Lu, J., Pei, G., Chan, L.S. (2006). Hybrid photovoltaic and thermal solar-collector designed for natural circulation of water. Applied Energy, 83(3): 199-210. https://doi.org/10.1016/j.apenergy.2005.02.007

[11] Fraisse, G., Ménézo, C., Johannes, K. (2007). Energy performance of water hybrid PV/T collectors applied to combisystems of Direct Solar Floor type. Solar Energy, 81(11): 1426-1438. https://doi.org/10.1016/j.solener.2006.11.017

[12] Yazdanifard, F., Ebrahimnia-Bajestan, E., Ameri, M. (2016). Investigating the performance of a water-based photovoltaic/thermal (PV/T) collector in laminar and turbulent flow regime. Renewable Energy, 99: 295-306. https://doi.org/10.1016/j.renene.2016.07.004

[13] Lenert, A., Wang, E.N. (2012). Optimization of nanofluid volumetric receivers for solar thermal energy conversion. Solar Energy, 86(1): 253-265. https://doi.org/10.1016/j.solener.2011.09.029

[14] Fudholi, A., Sopian, K., Yazdi, M.H., Ruslan, M.H., Ibrahim, A., Kazem, H.A. (2014). Performance analysis of photovoltaic thermal (PVT) water collectors. Energy Conversion and Management, 78: 641-651. https://doi.org/10.1016/j.enconman.2013.11.017

[15] Sharma, K.V., Sarma, P.K., Azmi, W.H., Mamat, R., Kadirgama, K. (2012). Correlations to predict friction and forced convection heat transfer coefficients of water based nanofluids for turbulent flow in a tube. International Journal of Microscale and Nanoscale Thermal and Fluid Transport Phenomena, 3(4): 1-25.

[16] Chandrasekar, M., Suresh, S., Senthilkumar, T. (2012). Mechanisms proposed through experimental investigations on thermophysical properties and forced convective heat transfer characteristics of various nanofluids–A review. Renewable and Sustainable Energy Reviews, 16(6): 3917-3938. https://doi.org/10.1016/j.rser.2012.03.013

[17] Ho, C.J., Liu, W.K., Chang, Y.S., Lin, C.C. (2010). Natural convection heat transfer of alumina-water nanofluid in vertical square enclosures: An experimental study. International Journal of Thermal Sciences, 49(8): 1345-1353. https://doi.org/10.1016/j.ijthermalsci.2010.02.013

[18] Xuan, Y., Roetzel, W. (2000). Conceptions for heat transfer correlation of nanofluids. International Journal of Heat and Mass Transfer, 43(19): 3701-3707. https://doi.org/10.1016/S0017-9310(99)00369-5

[19] Kalogirou, S.A. (2013). Solar Energy Engineering: Processes and Systems. Academic Press. https://doi.org/10.1016/B978-0-12-374501-9.X0001-5

[20] Duffie, J.A., Beckman, W.A., Blair, N. (2020). Solar Engineering of Thermal Processes, Photovoltaics and Wind. John Wiley & Sons. https://doi.org/10.1002/9781119540328

NOMENCLATURE

T	temperature, C
d_p	particle diameter, nm
k	nanofluid thermal conductivity, $W.m^{-1}.K^{-1}$
C	specific heat, J. $kg^{-1}.K^{-1}$
Q	useful heat gain, W
N_g	number of glass cover
h_w	forced convection, $W.m^{-2}.K^{-1}$
h_{fi}	fluid heat transfer coefficient, $W.m^{-2}.K^{-1}$
G_t	solar radiation, $W.m^{-2}$
$\dot{m}$	mass flow rate, $kg.s^{-1}$
A	area, m^2

Greek symbols

μ	viscosity, m.Pas
ϕ	volume concentration, vol.%
α	thermal diffusivity, m^2. s^{-1}

ρ	density, kg. m^{-3}
η	efficiency, %
τ_{pv}	pv transmittance
α_{pv}	pv absorptance
ε_g	glass emittance
ε_p	plate emittance
β	tilt angle, ^{o}

Subscripts

p	nanoparticle
w	base fluid (water)
nf	nanofluid
o	output
i	input
a	ambient
pv	photovoltaic
mn	mean plate
c	collector